Pis'ma v ZhETF, vol. 102, iss. 12, pp. 903 – 910

Multi-component quasi-elastic light scattering in $Na_{1/2}Bi_{1/2}TiO_3$ as studied by broadband Brillouin scattering

A. I. Fedoseev[+], *E. A. Popova*[+*], *P. P. Syrnikov*[+], *S. Kojima*[×], *S. G. Lushnikov*[+1)]

[+] *Ioffe Physical-Technical Institute of the RAS, 194021 St. Petersburg, Russia*

[*] *Department of Crystallography, St. Petersburg State University, 199034 St. Petersburg, Russia*

[×] *Institute of Materials Science, University of Tsukuba, 305-8573 Tsukuba, Japan*

Submitted 20 October 2015

Brillouin light scattering studies of the low-frequency region of vibrational spectra of a partially disordered ferroelectric crystal $Na_{1/2}Bi_{1/2}TiO_3$ (NBT) from 300 to 850 K are presented. It is shown that the light scattering spectra contain a multi-component quasi-elastic scattering (QELS) observed in a broad frequency range, from 800 to 0.7 GHz. Reconstruction of the inelastic light scattering spectra in NBT in the frequency region from 0.7 to 800 GHz did not reveal relaxation processes (α and β relaxations) typical of disordered compounds (glasses, supercooled liquids, etc.). The fractal approach also proved to be inapplicable to the description of QELS in NBT. Detailed analysis of the Brillouin spectra with different free spectral ranges ("frequency windows") showed that different contributions to the quasi-elastic light scattering manifest themselves in different "frequency windows". These contributions are associated with the structural phase transitions and other processes responsible for the emergence of QELS (domain structure evolution, heterophase fluctuations, etc.). Thus, we suggest a new approach to the analysis of the temperature behavior of quasi-elastic scattering. It allows one to study the critical dynamics of the crystal lattice and the nonphonon contributions into vibrational spectra of partially disordered crystals.

DOI: 10.7868/S0370274X15240029

Sodium bismuth titanate $Na_{1/2}Bi_{1/2}TiO_3$ (NBT) belongs to a large family of complex perovskites of the $A'A''BO_3$ type. The NBT crystal properties have been studied since the 1960s [1]. Recently they have attracted a considerable attention of researchers as "environmentally pure" compounds free of lead ions and having unique piezoelectric properties [2–3]. The crystal lattice dynamics of NBT remains a subject of discussion despite a long history of research. This is caused by the fact that the NBT properties strongly depend on the regime of temperature measurements (heating or cooling), probably on the method of crystal growth and, hence, on the degree of the A sublattice disordering. Numerous investigations of structural, dielectric, acoustic, optical, and other properties of NBT [3–18] allow one to propose the following sequence of phase transformations. In the high-temperature phase the NBT structure is cubic (O_h^1). At $T_1 \approx 820$ K (at cooling), a first-order ferroelastic phase transition to the tetragonal phase $P4bm$, $Z = 2$ occurs, and the phases coexist in the temperature interval of 20–30 deg. At $T_2 \approx 593$ K NBT passes into the rhombohedral phase $R3c$, $Z = 6$. This transition is accompanied by "wide" temperature anomalies in dielectric (with a low-frequency dispersion), acoustic and other macroscopic properties. At last, at $T_3 \approx 473$ K the NBT crystals pass into the ferroelectric state. "Wide" anomalies are typical of relaxor ferroelectrics, so NBT are also considered to be relaxors. In the low-temperature phase, the Raman spectra and IR spectra in the THz-frequency range exhibit an overdamped soft mode, traces of which are lost at $T \sim 300$ K, i.e., well below the ferroelectric phase transition temperature. It should be noted that recently the NBT structure and dynamics from 600 to 300 K have been widely discussed. The diffuse phase transition at $T_2 \approx 593$ K is attributed to the coexistence of tetragonal and rhombohedral phases [19, 20] in the region of 530–690 K. A characteristic feature of lattice dynamics in this temperature region is a strong diffuse scattering observed in neutron and X-ray scattering on the line connecting the R and M points of the Brillouin zone and the existence of a specific domain structure [5, 6, 10, 21]. The domain structure evolution in a wide temperature range was considered in detail in a number of publications [10, 21, 22]. The studies of the NBT microstructure by high-resolution electron microscopy has led the authors of [22] to the conclusion that there is

[1)] e-mail: Sergey.Lushnikov@mail.ioffe.ru

an intermediate, orthorhombic, phase that separates the tetragonal and rhombohedral phases. Antiferroelectric properties of the modulated phase also manifest themselves in this temperature range [19]. The unresolved problem is the existence of an isotropization point in the temperature transformations of NBT in the vicinity of $T \sim 580$ K, where the birefringence vanishes and changes the sign, and the domain structure disappears in the neighborhood of the isotropization point [10]. The structure of the ferroelectric phase in NBT still remains unclear. Both the rhombohedral and monoclinic symmetries and their coexistence are actively discussed [23].

The behavior of the NBT vibrational spectrum has been widely studied by Raman, Brillouin, IR [9, 12, 14–16, 24]. It has been shown that a characteristic feature of the light scattering spectra is the existence of quasi-elastic light scattering in the low-frequency region. The behavior of this scattering strongly depends on temperature and the mode coupling effect caused by the interaction of a low-lying transverse optical (TO) and acoustic phonons (TA) which manifests itself in the Brillouin scattering spectra as a distortion of the TA phonon line shape (the Fano effect) [14]. The quasi-elastic light scattering emerges at NBT heating in the vicinity of room temperatures simultaneously with the disappearance of the overdamped soft optical mode observed at low temperatures [15]. The quasielastic scattering manifests itself in the most pronounced manner in the temperature region 500–650 K in the vicinity of a broad maximum in the dielectric response [14, 15, 24]. Several authors attributed the temperature evolution of quasi-elastic light scattering to relaxation processes in NBT. Note that the quasi-elastic light scattering is a characteristic feature of vibrational spectra of many disordered perovskites. The nature of this scattering is not fully understood, but we believe that it plays a key role in the crystal lattice dynamics of these compounds.

Our analysis of the quasi-elastic scattering data for NBT obtained by optical spectroscopy has shown that it is multi-component. It can be supposed that its temperature behavior depends strongly on the "frequency window" in which measurements are carried out and reflects different processes in the crystal lattice dynamics of NBT. This necessitates detailed studies of the quasi-elastic light scattering in NBT crystals by broadband Brillouin light scattering in various "frequency windows".

Brillouin measurements were carried out on NBT single crystals grown by the Czochralski technique. The experiments were conducted in the 180° light scattering geometry, the object was an oriented plate $6 \times 5 \times 2\,\mathrm{mm}^3$ in size. The sample was oriented by an X-ray single-crystal diffractometer. The wave vector $\mathbf{q}_{ph}$ of the quasi-longitudinal acoustic phonon (QLA) observed in our experiments was along the [110] axis ($\mathbf{q}_{ph} \| [110]$) of the cubic phase. The excitation source of the scattered light was a single-frequency solid state laser ("Coherent") with the wavelength $\lambda = 532$ nm. The radiation power did not exceed 50 mW. The scattered light was analyzed with the help of a $(3+3)$ pass Fabry-Perot interferometer (J. Sandercock tandem) equipped with an optical microscope. For temperature measurements the samples were mounted in a cell (Linkam THMS 6000), where the temperature was lowered from 870 to 300 K, with a stabilization in the limits of ± 0.1 K. To study the behavior of the quasi-elastic light scattering in different "frequency windows", different free spectral ranges of the interferometer (FSR) (6, 12, 100, 800 GHz) were used. According to the fluctuation-dissipation theorem, the spectral function is proportional to the imaginary part of susceptibility $\chi''(\omega)$:

$$S(\omega) \approx \frac{k_{\mathrm{B}}T}{\hbar\omega}\chi''(\omega) \quad \text{for} \quad \hbar\omega \ll k_{\mathrm{B}}T, \tag{1}$$

$$\frac{T}{I_{CP}} \propto \left(\int_0^\infty \frac{\chi''(\omega)}{\omega} d\omega \right)^{-1} \propto \chi'(0)^{-1}, \tag{2}$$

where k_{B} is the Boltzmann constant and T is the temperature in Kelvins. Thus, the integral intensity of quasi-elastic scattering I_{CP} in the Brillouin spectra is proportional to the static real susceptibility $\chi'(0)$ at the lowest frequency limit of Brillouin scattering. The quasi-elastic component contour is well described by a Lorentzian, and the excitation is a Debye relaxor. By measuring the quasi-elastic component full-width at half-maximum Γ (FWHM) we can estimate the relaxation time $\tau = 1/\pi\Gamma$.

The Brillouin scattering spectra with FSR of 100 and 800 GHz exhibited a QLA phonon, the velocity (V) of which was determined by a linear combination of elastic constants C_{11}, C_{33}, and C_{12} (cubic phase). Note that according to the X-ray data [4] the ratio between cell parameters in NBT changed only slightly during phase transitions, $a/c = 0.999$ at T_1 and decreased to 0.998 at T_2. For this reason, the description of its acoustic properties above room temperature in which we are interested will be given in the pseudocubic approximation. The acoustic phonon velocity in a Brillouin light scattering experiment is determined by the frequency shift ($\Delta\nu$) as $Vq = \omega = 2\pi\Delta\nu$, $q = (4\pi n/\lambda)\sin(\theta/2)$, where q, n, and θ are the wavevector, refractive index, and angle between the incident and scattered light, respectively. The spectra obtained were processed by the

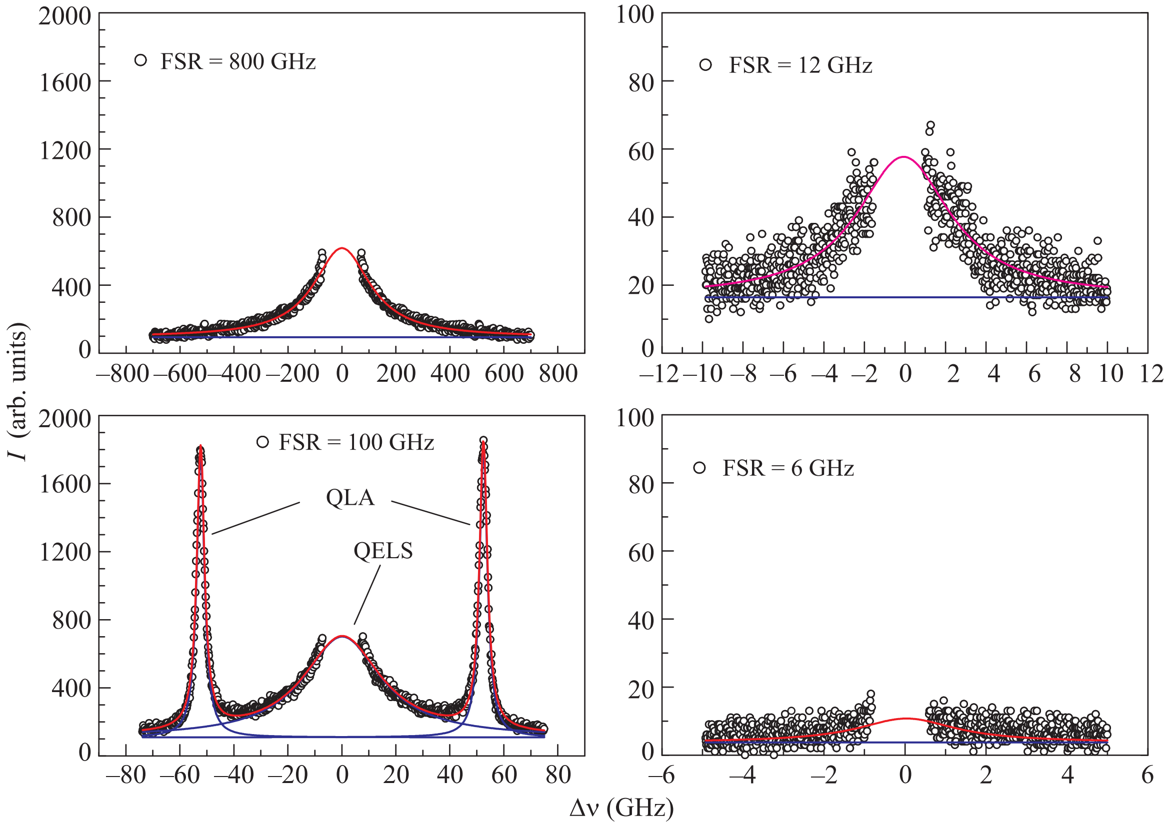

Fig. 1. (Color online) Brillouin light scattering spectra for NBT in various "frequency windows" (with different FSR) at $T = 603$ K. The thick blue and red lines show results of spectrum fitting

method of least squares. As fitting functions in the calculations of contours of phonon lines, the damped harmonic oscillator function was used. To take into account the exciting line (instrumental function), the Gaussian function was employed. The calculations yielded temperature dependences of the integral intensity, full-width of QELS and QLA phonon and also the phonon frequency shift proportional to the hypersonic phonon velocity. Examples of experimental spectra for different FSR and fitting results are presented in Fig. 1.

To analyze the quasi-elastic scattering in disordered compounds, such as glasses, supercooled liquids, relaxor ferroelectrics of the $PbMg_{1/3}Nb_{2/3}O_3$ (PMN) type, etc., the so-called combined spectra of inelastic light scattering obtained by Brillouin and Raman spectroscopy are widely used [25–27]. This makes it possible to analyze the behavior of different relaxation processes such as, for example, α and β relaxations in glasses and supercooled liquids [25, 26]. As in the case of relaxor ferroelectric PMN, combined scattering spectra were also used to apply the fractal approach to the analysis of the QELS behavior in the low-frequency dynamics of the vibrational spectrum [27].

We used the Brillouin scattering spectra obtained for NBT during experiments with different FSR to construct combined spectra which cover frequency region from 0.7 to 700 GHz. Fig. 2 shows examples of the combined spectra at different temperatures at the double logarithmic scale. First of all, it should be noted that there are no manifestations of specific relaxation processes, such as α and β relaxation in glasses (compare Fig. 2 and Figs. in [25, 26]) in the combined spectra of NBT, as well as of PMN (compare Fig. 2 and Fig. 3 in [27]). Thus, disordering in the A or B sublattices of cubic relaxor ferroelectrics does not cause characteristic "glass" processes in the vibrational spectrum. We used the approach suggested by the authors of [27] who described the quasi-elastic light scattering in PMN in the framework of the fractal approach and conducted approximation of combined scattering spectra by power function $I(\omega) \sim \omega^{\alpha}$. The power-low spectrum intensity can be expressed as a superposition of many Lorentzian spectra. This approach proved to be quite efficient for PMN. The approximation of this type allows one to obtain a characteristic value the behavior of which shows the evolution of quasielastic light scattering with tem-

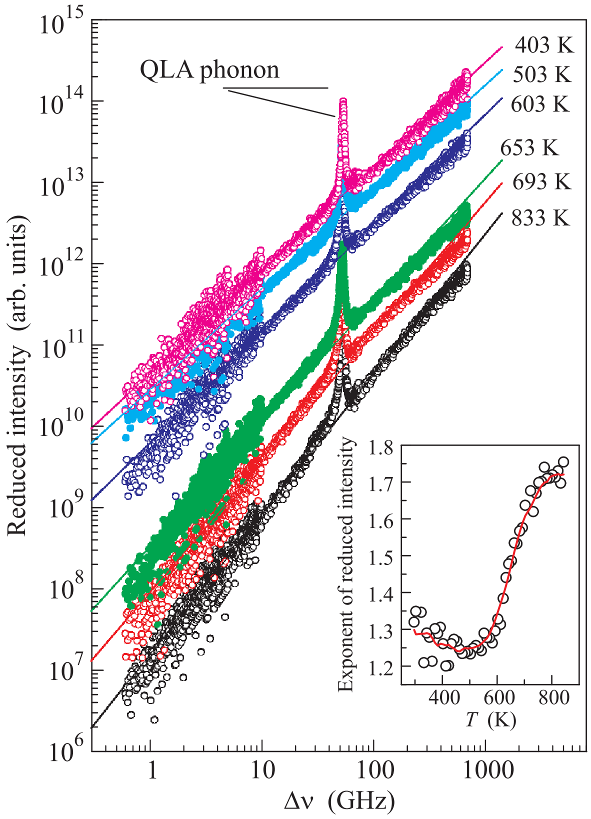

Fig. 2. (Color online) The reduced intensity $I(\nu)$ for NBT at different temperatures. The spectra are vertically shifted only by multiplication of constant for visual clarity. The solid lines present the fits of the power function as described in the text. The inset shows temperature dependence of the power exponent of the reduced intensity for NBT

perature. In the case of NBT we could not correctly approximate the $I(\omega)$ function by the power function. It can be seen from Fig. 2 that the experimental points deviate from the results of approximation in the low- and high-frequency regions of the combined spectra. However, the temperature dependence of the exponent shown in the inset to Fig. 2 is in good agreement with such a temperature dependence of PMN [27]. The deviations from the approximation results indicate evidently that there are additional contributions to the quasi-elastic light scattering. To find these contributions into the QELS, we analyzed the temperature evolution of quasi-elastic scattering in different "frequency windows".

Let us first consider the behavior of the Brillouin light scattering spectra at FSR = 800 GHz. Fig. 3 shows results of fitting of the data for the quasi-elastic scattering alone because the calculations for the acoustic phonon at this FSR give a big error. The temperature dependences of the integral intensity and full-width Γ

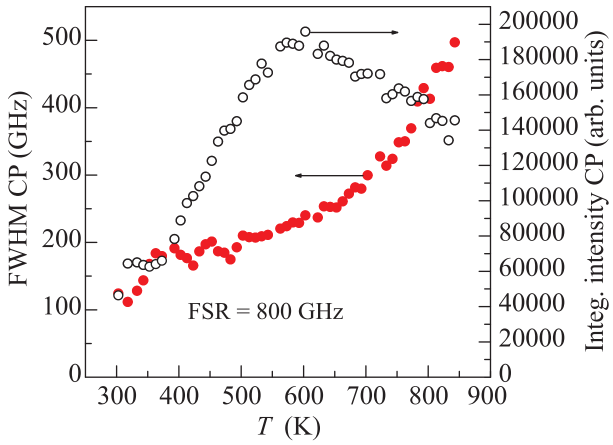

Fig. 3. (Color online) Temperature dependences of the full-width at half-maximum (FWHM) and integrated intensity of QELS for NBT in Brillouin spectra with FSR = 800 GHz

of the quasi-elastic scattering are shown in Fig. 3. The figure clearly shows that the QELS susceptibility increases with decreasing temperature, reaches a maximum in the vicinity of 580 K (near the maximum of the dielectric permeability – T_m), and then gradually falls as the temperature further decreases. The QELS full-width decreases monotonically with decreasing temperature without any anomalies in the vicinity of 580 K. In the vicinity of 480 and 430 K, weak anomalies are observed. Below 350 K the $\Gamma(T)$ decreases sharply (from 200 to 100), and the QELS susceptibility is constant in this temperature region (Fig. 3). It should be noted that the QELS full-width observed in this "frequency window" is in good agreement with the half-width at half-maximum (HWHM = 0.5FWHM) of the narrow central peak in the Raman scattering discovered in [24]. However, we could not describe its temperature behavior in terms of the Arrhenius or Vogel–Fulcher law, as in [24]. The magnitudes of activation energy and freezing temperatures obtained in the calculations were nonphysical. This difference in the behaviors of QELS in Raman and Brillouin light scattering can be explained by the difficulties encountered in fitting the data in the Raman spectra at deconvolution of the QELS components and resulting large errors. Analysis of Brillouin data gives a much more accurate picture of the QELS behavior. The processes responsible for the temperature behavior of QELS in this "frequency window" are not thermally activated in the sense defined by the Arrhenius and Vogel–Fulcher law.

The Brillouin light scattering spectra for FSR = 100 GHz include well-described acoustic phonons and quasi-elastic light scattering (see Fig. 1). The acoustic phonon behavior did not exhibit a mode-coupling phenomenon, similar to [14]. In this experimental geometry no resonance distortions of the line shape were observed in the entire temperature range studied. This enabled fitting of the data by using a sum of a damping harmonic oscillator (QLA phonon) and Lorenz function (QELS). One of the additional parameters that was taken into account in fitting of the experimental scattering spectra was the background the behavior of which also varied with temperature (see Fig. 4a). Figs. 4b and c show temperature dependences of the

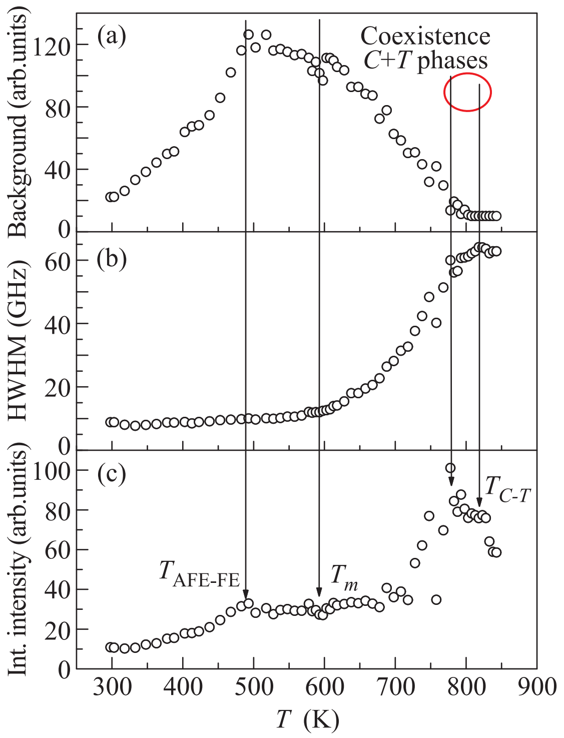

Fig. 4. (Color online) Temperature dependences of the background intensity (a), the half-width at half-maximum (b), and integrated intensity of QELS (c) in NBT in the Brillouin spectra with FSR = 100 GHz

half-width at half-maximum (HWHM) and susceptibility of QELS. It is clearly seen that both parameters exhibit anomalies in the vicinity of 820 K (near the phase transition from cubic to tetragonal phase) and at 775 K, where the susceptibility reaches a maximum, while the HWHM begins to decrease monotonically, reaching a minimum in the vicinity of 580 K below which it becomes temperature-independent. The QELS susceptibility sharply decreases when temperature decreases to 700 K (relative to the value near 780 K, it is 3 times as low). From this temperature and up to 500 K it weakly depends on temperature. A further decrease in temperature results in a non-linear and monotonic decrease in the susceptibility. Of great interest is the temperature behavior of the background in the scattering spectra (see Fig. 4a). In the cubic phase of NBT the background is nearly independent of temperature and is at a minimum. Below 800 K, i.e., after the ferroelastic phase transition, the background begins to grow, and after this the temperature dependence exhibits two anomalies in the vicinity of 600 and 500 K. A further decrease results in the background reduction at room temperature to the values slightly higher than those observed in the cubic phase of NBT. It is worth saying here that the background in the Brillouin scattering spectra of NBT is actually a manifestation of QELS which we observe in a wide "frequency window". In other words, it is a maximum of the broad component of quasi-elastic scattering which was analyzed for FSR = 800 GHz, and the temperature dependence of the background mainly reflects the behavior of the susceptibility of this component. The anomalies observed in the vicinity of 600 and 500 K are rather weak and apparently are not visible at large FSR.

The temperature behavior of the frequency shift, half-width at half-maximum, and integral intensity of the quasi-longitudinal acoustic phonons in the scattering spectra with FSR = 100 GHz are shown in Fig. 5. In general, the behavior of the phonon frequency shift and the half-width are similar to those reported in [12], i.e., there are a broad minimum of the frequency shift ($\Delta\nu$) and a wide maximum of the half-width at half-height, with extremes in the vicinity of 580 K, which corresponds to the maximum dielectric response in NBT. A similar dependence was observed in PMN [28]. However, in contrast to PMN, we see additional anomalies in the acoustic phonon behavior. Fig. 5 clearly shows that the temperature dependence $\Delta\nu(T)$ has small kinks in the vicinity of 810 and 780 K, here weak anomalies in damping and intensity of QLA are also observed. These anomalies correspond to a phase transition from the cubic to the tetragonal phase and the region of phase coexistence. The intensity of the QLA phonon has an anomaly in the vicinity of 700 K. This anomaly does not manifest itself in the temperature dependence of the half-width and frequency shift. A step-like decrease in the intensity by 25 % may be due to changes in the photoelastic constants responsible for the intensity of the Brillouin doublet in the scattering spectra [29] and is caused, apparently, by the domain structure evolution in this temperature range. This hypothesis is based on the absence of anomalies in the behavior of the frequency shift and half-width of QLA phonons. In the vicinity of 600 K the temperature dependence of the QLA frequency has a weak jump to which a wide maximum

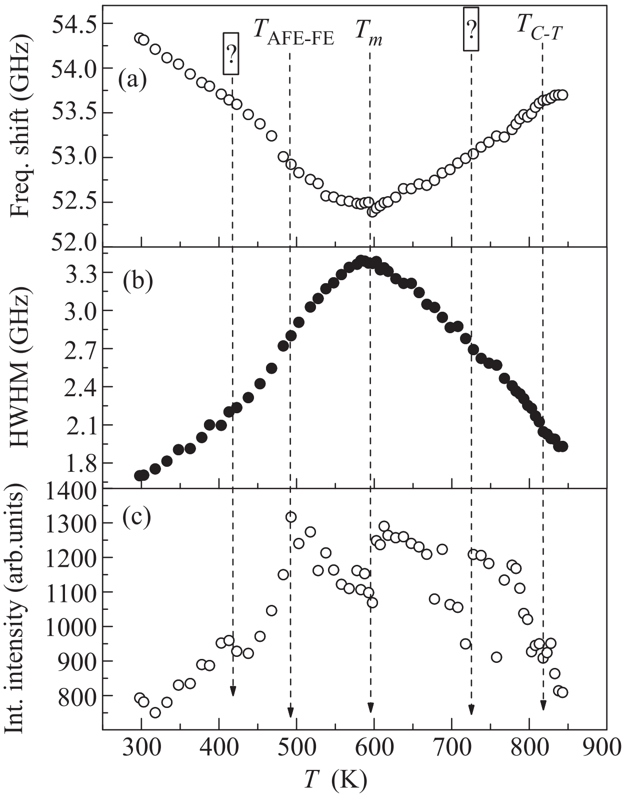

Fig. 5. Temperature dependences of the frequency shift $\Delta\nu$ (a), half-width at half-maximum (b), and integrated intensity (c) of the quasi-longitudinal acoustic phonons with $\mathbf{q}_{ph}\|[110]$ in NBT in the Brillouin spectra with FSR = 100 GHz

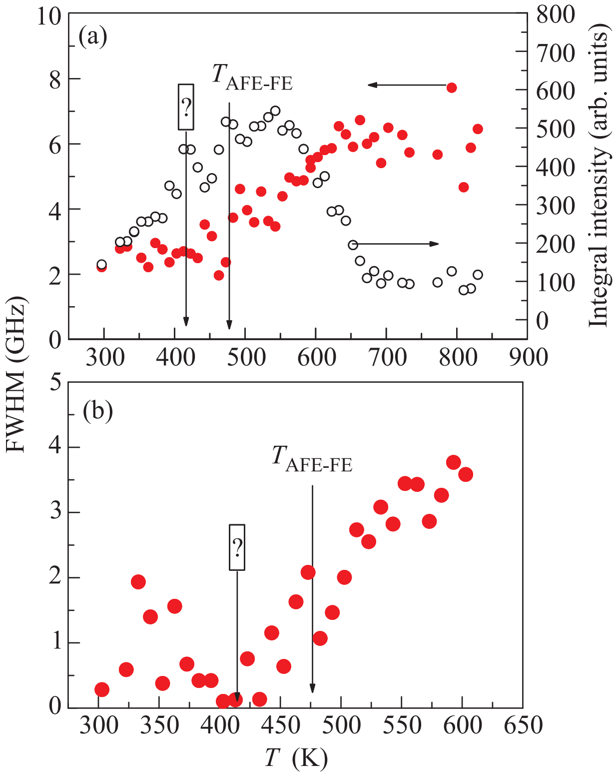

Fig. 6. (Color online) Temperature dependences of the full-width at half-maximum and integrated intensity of QELS in NBT in Brillouin spectra with FSR = 12 GHz (a) and full-width at half-maximum of QELS in the scattering spectra with FSR = 6 GHz (b)

of damping and a sharp drop in the phonon intensity correspond. A further temperature decrease leads to a frequency increase and a wide anomaly near 480 K, to which the intensity growth with a maximum near 480 K corresponds. It should be noted that the anomalies in the temperature evolution of QELS and QLA phonon correlate well with each other in the vicinity of the transition from the cubic to the tetragonal phase and in the vicinity of 500 K. This suggests that they are due to the NBT lattice dynamics.

In the Brillouin spectra with FSR = 12 and 6 GHz the acoustic phonon contribution into the structural dynamic factor being analyzed is minimal because its frequency ($\Delta\nu \sim 52$ GHz) is much higher than the "frequency window" used. The QELS behavior in the spectra with FSR = 12 GHz is shown in Fig. 6a. The figure clearly shows that above 670 K the QELS behavior is nearly independent of temperature. Starting from 650 K, as temperature is decreased, the QELS full-width monotonically decreases, and the susceptibility increases and reaches a maximum in the vicinity of 550 K. A similar maximum shifted by 50 deg towards higher temperatures was also observed in the temperature behavior of the susceptibility of QELS in a large frequency window (FSR = 800 GHz). The temperature dependences of both the full-width and susceptibility have pronounced anomalies in the vicinity of 480 and 420 K which were found in the analysis of Brillouin spectra with FSR = 800 GHz. Below 400 K, the QELS full-width becomes temperature-independent, and the QELS susceptibility decreases monotonically. It is difficult to analyze the Brillouin spectra with FSR = 6 GHz because it is actually the limiting regime in which the 3 + 3 pass tandem Fabry–Perot interferometer can operate. The intensity of the scattering spectra is very low, and the accumulation of spectra leads only to an increasing error. The QELS intensity is low, and it is difficult to see it in the Brillouin spectra. Therefore, in Fig. 6b we present only changes in the QELS full-width. As the quantitative evaluation shows, $\Gamma(T)$ of QELS remains nearly unchanged as temperature falls to 550 K, then $\Gamma(T)$ decreases in the temperature range 550–450 K, and after this it again becomes independent of temperature.

Thus, the results obtained in our study show that combined Brillouin light scattering spectra do not allow one to analyze in detail the QELS behavior in the case of NBT. When temperature varies, the QELS exhibits different behaviors in different frequency ranges of measurements ("frequency windows"). In the case of a wide "frequency window" (800 GHz), as well as in combined spectra, we actually see the integral picture in which the contribution of lattice dynamics is poorly distinguished. The maximum in the QELS susceptibility is consistent with a broad maximum in the permittivity of NBT near 550 K, as in the case of PMN. Possibly, the emergence of QELS in NBT and also changes in its temperature behavior have the same mechanisms as the behavior of permittivity in the vicinity of the diffuse phase transition.

We observe, apparently, two processes in the scattering spectra of NBT with FSR = 100 GHz. The first is due to the critical dynamics in the vicinity of the ferroelastic phase transition from the cubic to the tetragonal phase, and the second is associated with the domain structure formed in the vicinity of 470 K, where, as the authors of [19] believe, the antiferroelectric modulated phase ends and the remanent polarization vanishes. This phase also manifests itself in the behavior of the acoustic phonon in the form of anomalies in the temperature dependences of the shift and susceptibility in the vicinity of 590 and 470 K. The nature of the anomaly near 420 K observed in both the narrow and wide frequency ranges (FSR = 6, 12, and 800 GHz, respectively) is still unclear. The QELS behavior in NBT in the narrow "frequency window" (12 and 6 GHz) most probably reflects the evolution of structures at the mesoscales in the antiferroelectric modulated phase because the anomalies in susceptibility and full-width are limited by the interval of 650–450 K. It is rather difficult to speak about the exact boundaries of the existence of the modulated antiferroelectric phase because characteristic temperatures depend on both the heating-cooling regime and the sample prehistory (growth technique, annealing, etc.). However, it is absolutely clear that different processes associated with the critical lattice dynamics and other possible mechanisms, such as rearrangement of the domain crystal structure and/or movement of domain walls, heterophase fluctuations arising in the region of phase coexistence and their evolution, etc., manifest themselves in the narrow, medium and wide "frequency windows" (FSR = 6 and 12; 100, 800 GHz, respectively). The goal of our study was not to identify possible mechanisms of quasi-elastic light scattering. This requires a set of additional measurements, including those that allow one to find the dependence of the QELS width on q. We showed at this stage of investigations, by using NBT as an example, that partially disordered ferroelectrics and related compounds can give rise to multi-component QELS that occupies a wide frequency region in the vibrational spectrum of the crystal. We suggest the approach that allows a correct analysis of different contributions into the multi-component quasi-elastic light scattering.

The authors wish to thank S.N. Gvasaliya for fruitful discussions. The investigations were supported by Russian Science Foundation (project # 14-12-00257).

1. G. A. Smolensky, V. A. Isupov, A. I. Agranovskaya, and N. N. Kraynik, Fiz. Tverd. Tela **11**, 2982 (1960).
2. S. M. Emelyanov, I. P. Raevskiy, V. G. Smotrakov, and F. I. Savenko, Fiz. Tverd. Tela **26**, 1897 (1984).
3. K. Rodeler, I. Franke, A. M. Glazer, P. A. Thomas, S. Miga, and J. Suchanicz, J. Phys.: Cond. Mat. **14**, 5399 (2002).
4. G. O. Jones and P. A. Thomas, Acta Cryst. B **58**, 168 (2002).
5. A. M. Balagurov, E. Yu. Koroleva, A. A. Naberezhnov, V. P. Sakhnenko, B. N. Savenko, N. V. Ter-Oganessian, and S. B. Vakhrushev, Phase Trans. **79**, 163 (2006).
6. B. N. Rao, R. Datta, S. S. Chandrashekaran, D. K. Mishra, V. Sathe, A. Senyshyn, and R. Ranjan, Phys. Rev. B **88**, 224103 (2013).
7. C.-S. Tu, I. G. Siny, and V. H. Schmidt, Phys. Rev. B **49**, 11550 (1994).
8. F. Cordero, F. Craciun, F. Trequattrini, E. Mercadelli, and C. Galassi, Phys. Rev. B **81**, 144124 (2010).
9. J. Petzelt, S. Kamba, J. Fabry, D. Noujni, V. Porokhonskyy, A. Pashkin, I. Franke, K. Roleder, J. Suchanicz, R. Klein, and G. E. Kugel, J. Phys.: Cond. Mat. **16**, 2719 (2004).
10. M. Geday, J. Kreisel, A. M. Glazer, and K. Roleder, J. Appl. Crystallogr. **33**, 909 (2000).
11. V. R. Mudinepalli, N. R. Reddy, W.-C. Lin, K. V. Siva Kumar, and B. S. Murty, Adv. Mater. Lett. **6**, 27 (2015).
12. I. G. Siny, C.-S. Tu, and V. H. Schmidt, Phys. Rev. B **51**, 5659 (1995).
13. J. Suchanicz, J. Mat. Sci. **37**, 489 (2002).
14. A. I. Fedoseev, S. G. Lushnikov, S. N. Gvasaliya, P. P. Syrnikov, and S. Kojima, Phys. Sol. State **51**, 1399 (2009).
15. I. G. Siny, E. Husson, J. M. Beny, S. G. Lushnikov, E. A. Rogacheva, and P. P. Syrnikov, Ferroelectrics **248**, 57 (2000).
16. J. Kreisel, A. M. Glazer, G. Jones, P. A. Thomas, L. Abello, and G. Lucazeau, J. Phys.: Cond. Mat. **12**, 3567 (2000).
17. G. Deng, S. Danilkin, H. Zhang, P. Imperia, X. Li, X. Zhao, and H. Luo, Phys. Rev. B **90**, 134104 (2014).
18. K. Sakata and Y. Masuda, Ferroelectrics **7**, 347 (1974).

19. V. Dorcet, G. Trolliard, and P. Boullay, J. Mag. Mag. Mat. **321**, 1758 (2009).
20. R. Beanland and P. A. Thomas, Scripta Mat. **65**, 440 (2011).
21. R. Beanland and P. A. Thomas, Phys. Rev. B **89**, 174102 (2014).
22. V. Dorcet, G. Trolliard, and P. Boullay, Chem. Mat. **20**, 5061 (2008).
23. S. Gorfman and P. A. Thomas, J. Appl. Crystallogr. **43**, 1409 (2010).
24. D. K. Jackson, J. Toulouse, and H. Luo, Phys. Rev. B **90**, 054108 (2014).
25. V. N. Novikov, N. V. Surovtsev, J. Wiedersich, S. Adichtchev, S. Kojima, and E. Reossler, Europhys. Lett. **57**, 838 (2002).
26. G. Li, W. H. Du, X. K. Chen, H. Z. Cammins, and N. J. Tao, Phys. Rev. A **45**, 3867 (1992).
27. A. Koreeda, H. Taniguchi, S. Saikan, and M. Itoh, Phys. Rev. Lett. **109**, 197601 (2012).
28. R. A. Cowley, S. N. Gvasaliya, S. G. Lushnikov, B. Roessli, and G. M. Rotaru, Adv. Phys. **60**, 229 (2011).
29. R. Vacher and L. Boyer, Phys. Rev. B **6**, 639 (1972).